

# Dynamics of molecules confined in nanocages. A deuteron NMR study at high temperature

A. Birczyński and Z. T. Lalowicz\*

*H. Niewodniczański Institute Nuclear Physics PAS, ul. Radzikowskiego 152, 31-342*

*Kraków, Poland*

E-mail: Zdzislaw.Lalowicz@ifj.edu.pl

Phone: +48 12 6628259. Fax: +48 12 6628458

## Abstract

Our published and new experimental results by means of deuteron NMR spectroscopy in studies of molecular mobility in confinement are summarized and analysed. Conclusions about limits of applicability of methods in disclosing several features are achieved. A set of molecules:  $D_2$ ,  $CD_4$ ,  $D_2O$ ,  $ND_3$ ,  $CD_3OD$  and  $(CD_3)_2CO$  was chosen and introduced into zeolites with faujasite structure. Measurements of deuteron spectra and relaxation in function of loading and temperature provide a wealth of cases. A transition from translational into rotational mobility on decreasing temperature was a common observation. Fast magnetization exchange between two subsystems with different mobility was considered as a model. Existence of  $D_2O$  clusters and trimers of  $CD_3OD$  was a particularly significant evidence for importance of mutual interactions. Evolution of spectral components, derivation of the activation energy and  $T_1/T_2$  ratio are among analysed features. Choice of the zeolite, eg. NaY or NaX, introduces specific interactions with the zeolite framework. Temperature at which molecules become immobilized on cage walls is related to the strength of the interactions. On increasing temperature we may observe features like for layers of liquid on cage walls and gaseous state. In general properly chosen molecules may be used for characterization of host microporous systems.

Keywords: water clusters, hydrogen bonding, molecular dynamics, activation energy, phase transition, hysteresis

# Introduction

Recent review articles prove continuous importance of porous media and their applications. Buntkowsky et al.<sup>1</sup> outlined applicability of NMR technique ( $^{15}\text{N}$  and  $^2\text{H}$  spectroscopy, MAS NMR, NMR diffusometry) for studies of the molecules dynamics in confinement reflecting a wealth of interactions. Some more aspects were summarized in a more recent review from the same group.<sup>2</sup> NMR-crystallography, isotopically-labelled materials, NMR spectra of paramagnetic microporous materials and other methods discussed in,<sup>3</sup> may guide studies of substrates. We concentrate in our approach on deuteron NMR studies of selected molecules confined in cages of zeolites with faujasite structure.

Zeolites are porous inorganic crystals basically with the atomic formula  $\text{TO}_2$ , where the oxygens are arranged tetrahedrally around the central atom T (T represents silicon or aluminum atoms in the more common zeolites). Zeolite Y of the faujasite type has a well defined pore system. The supercages of 1.16 nm inner diameter are interconnected by 12-oxygen rings of 0.74 nm diameter. Moreover, there are also smaller sodalite cages of inner diameter of 0.66 nm connected to supercages by windows of 0.25 nm diameter formed by 6-oxygen rings. The unit cell of Y zeolite consists of eight supercages and eight sodalite cages and contains 192 T atoms and 384 oxygen atoms.<sup>4</sup>

Hydroxyl protons in zeolite HY are attached to oxygens bridging tetrahedrally coordinated silicon and aluminum atoms. These protons compensate the negative framework charges introduced by tetrahedrally coordinated aluminums, alternatively the same role is played by sodium cations. Thus OH groups are named as structural or bridging OH groups ( $\text{SiOHAl}$ ). In real crystals some imperfections can be found in a form of silanol ( $\text{SiOH}$ ) groups or OH groups associated with some extra-framework aluminum species.<sup>5</sup>

The unit cell of zeolite Y contains 384 oxygen atoms at four crystallographically inequivalent positions from O1 to O4. One can therefore expect four different types of bridging hydroxyl groups with protons at the positions from H1 to H4. The protons H1 and H4 point into supercages while the protons H2 and H3 are directed towards the 6-oxygen rings.

Czjzek et al.<sup>6</sup> used neutron diffraction to determine the following abundances of protons at respective positions in the unit cell:  $n(1) = 28.6$ ,  $n(2) = 9.5$  and  $n(3) = 15$  in zeolite HY (Si/Al = 2.4). No H4 protons were detected. The positions H1 and H3 are occupied preferentially and that confirms the results of quantum mechanical calculations.<sup>7,8</sup>

## Theory

Deuteron NMR is particularly suitable for the investigation of molecular mobility for a number of reasons. First, the quadrupole coupling constant is two orders of magnitude larger than the dipole-dipole coupling constant for protons. Second, the value of the quadrupole coupling constant depends on deuteron location and may provide information on the local structure and bonding. Third and most importantly, since the quadrupole coupling involves only one spin, information on molecular reorientation is not affected by the presence of neighboring nuclei. Therefore, motional averaging of the quadrupole interaction allows the clear discrimination between possible motional models.<sup>9</sup>

Molecular reorientations rendering the quadrupole interaction time-dependent and inducing transitions between nuclear Zeeman levels drive the deuteron NMR relaxation. The spin-spin and spin-lattice relaxation rate constants are given as different linear combinations of spectral density functions weighted by the coefficient  $A = (3/10)\pi^2 C_Q^2$ , where quadrupolar coupling constant  $C_Q = e^2 q Q / h$ . In the simplest case of isotropic diffusion characterised by exponential autocorrelation function with a single correlation time  $\tau_c$ , the spin-lattice relaxation rate constant is given by:<sup>10</sup>

$$R_1 = \frac{1}{T_1} = A [J(\tau_c, \omega_0) + 4J(\tau_c, 2\omega_0)], \quad (1)$$

where  $J(\tau_c, \omega_0) = \tau_c / (1 + \tau_c^2 \omega_0^2)$  is the spectral density function, being the Fourier transform of the autocorrelation function, with  $\omega_0 / 2\pi$  equal to the Larmor frequency. The correlation time  $\tau_c$  is assumed to follow the Arrhenius formula  $\tau_c = \tau_0 \exp(E_a / kT)$  with the activation

energy  $E_a$ . The temperature dependence of the relaxation rate has an inverted V shape with the maximum at temperature fulfilling the condition  $\omega_0\tau_c = 0.616$  which leads to

$$\left(\frac{1}{T_1}\right)_{max} = 1.425 \frac{A}{\omega_0}. \quad (2)$$

Fast motions, obeying  $\omega_0\tau_c \ll 1$ , contribute to the high temperature side of the maximum, while the low temperature side represents the relation  $\omega_0\tau_c \gg 1$ . The slopes, in some cases unequal, provide the value of the activation energy  $E_a$ . Moreover, the value of  $\tau_0$  and  $C_Q$  can be calculated from the known position of the maximum and its absolute value.

In the following a spin system will be assumed to consist of two subsystems characterized by a fast and slow motional regime with intrinsic relaxation rates  $R'_1$  and  $R''_1$ , respectively. In the limit of the fast magnetization exchange between the subsystems a single apparent relaxation rate can be observed:<sup>11</sup>

$$R_1 = WR'_1 + (1 - W)R''_1, \quad (3)$$

where  $W$  depends on relative abundances of molecules in both subsystems and  $R'_1$  and  $R''_1$  are expressed by eq 1, however for different correlation times. Experimentally, the limit of the applicability of eq 3 is described by the temperature  $T_S$ . Above  $T_S$  narrow deuteron NMR lines are observed. Below  $T_S$  a substantial, step-wise broadening of deuteron spectra appears, and magnetization recovery becomes nonexponential.<sup>12</sup>

Generally, NMR spectra are sensitive to molecular reorientations on the NMR time scale,<sup>13,14</sup> which is reflected in the condition for the narrowing of spectra expressed as  $\delta\tau_c \sim 1$ , where  $\delta$  is the width of a given spectrum and  $\tau_c$  is the temperature-dependent correlation time. For a typical width of a deuteron spectrum,  $\delta = 135$  kHz for  $C_Q = 180$  kHz, the condition  $\delta\tau_c \sim 1$  leads to the correlation time  $\tau_c = 10^{-6}$  s. For  $\tau_c \gg 10^{-6}$  s deuterons are considered to be immobile and the Pake doublet is observed. The doublet separation equals  $(3/4)C_Q$ , which can be used to provide the value of the quadrupole coupling constant.

Narrowed spectra result for  $\tau_c \ll 10^{-6}$  s. Deuteron NMR spectra are inhomogeneous<sup>15</sup> and consist of the doublets covering the whole spectral range. The doublets undergo motional narrowing sequentially at somewhat different temperatures for differently oriented deuterons. For example, deuteron NMR spectra of polycrystalline  $\text{ND}_4\text{VO}_3$  measured between 60 K and 83 K were found to be sensitive to correlation frequencies in the range 210 kHz to 1 kHz (corresponding to correlation times in the range  $7.6 \times 10^{-7} \text{ s} \leq \tau_c \leq 1.6 \times 10^{-4} \text{ s}$ ).<sup>16</sup> This result shows that the range of molecular mobilities, where the spectra can be considered to be in the intermediate narrowing regime, is quite broad.<sup>17,18</sup>

## Experimental

Zeolites NaX (supplied by Sigma–Aldrich) and NaY (purchased from Linde company) were activated *in situ* in an NMR cell. First, samples were evacuated at room temperature for 30 min, then temperature was raised with the rate 5 K/min up to 700 K and kept at this temperature in vacuum for 1 h. The doses of selected compounds were sorbed in zeolites NaX and NaY up to 100% and 200%, of the total coverage of  $\text{Na}^+$  ions. The samples were sealed in 24 mm long glass tubes with the outside diameter 5 mm.

The NMR experiments were carried out over a range of temperatures regulated by the Oxford Instruments CT503 Temperature Controller to the accuracy of  $\pm 0.1$  K. The static magnetic field 7 T was created by the superconducting magnet made by Magnex, and the  $^2\text{H}$  resonance frequency was equal to 46 MHz. The NMR probe was mounted inside the Oxford Instruments CF1200 Continuous Flow Cryostat. Pulse formation and data acquisition were provided by Tecmag Apollo 500 NMR console. The dwell time was set to  $2 \mu\text{s}$ . The  $\pi/2$  pulse equal to  $3 \mu\text{s}$  assured the uniform excitation<sup>19</sup> for our 200 kHz spectra.

NMR spectra were obtained by the Fourier transformation of the free induction decay (FID). For eliminating spectral baseline distortion an extension<sup>20</sup> of Heuers method<sup>21</sup> dedicated to wide spectra was used. The nature of quadrupole interaction for deuterons allows

us to expect symmetric spectra. Thus, the zeroing of the imaginary signal was possible at the final stage of signal processing. An acceptable signal-to-noise ratio in the spectra was achieved by signal averaging over several thousands of accumulations depending on loading. Repetition time was kept at least 5 times longer than the time constant observed in relaxation.

NMR spectra were obtained by the Fourier Transformation of the Free Induction Decay (FID) or Quadrupole Echo (QE) signal for narrow and broad ones, respectively. For the FID and QE spectra the sequences  $(\pi/2)_x-t$  and  $(\pi/2)_x-\tau-(\pi/2)_y-t$  were used with separation time  $\tau$  of the order of  $50\text{ }\mu\text{s}$  in the QE sequence. The pulse separation time  $\tau$  was adjusted by means of the home-designed code for Tecmag console in order to optimize QE signal intensity for each temperature. The phase cycling sequence was applied and focused on the FID signal cancellation in the overall signal after the quadrupole echo sequence.

## Results and discussion

Nuclear magnetic resonance provides means to study molecular dynamics in every state of matter. Molecules in confinement provide a particularly rewarding system as with a single sample we may observe on increasing temperature immobilized molecules, then onset of molecular reorientation and, in some cases, translational diffusion. We selected a set of molecules with diverse properties leading to a wealth of specific features in mobility. We restrict ourselves to zeolites of faujasite structure and have a common environment in terms of size and structure.

### $\text{D}_2$ and $\text{CD}_4$

Spin-lattice relaxation rate was measured for zeolite NaY with one  $\text{D}_2$  molecule per supercage in the range 310 K to 66 K. The theory of deuteron spin-lattice relaxation for free  $\text{D}_2$  quantum rotators was developed leading to successful fits.<sup>22</sup> Relaxation rates were calculated for ortho-

D<sub>2</sub> and para-D<sub>2</sub>. The spin-rotational interaction as well as quadrupole and dipole-dipole interactions under interference condition were taken into account. Relaxation rates were derived as weighted sums of contributions from rotational states according to their Boltzmann population. In result of that we observed that relaxation rates surpass values defined by the quadrupole coupling constant. That is unique case. The low temperature slope of the relaxation rate was observed at temperature above 110 K, indicating  $\omega_0\tau_c \gg 1$  condition, thus long correlation times. Molecules diffuse freely in the space of cages. Only collisions, among them and with cage walls, change their orientation. Many collisions are necessary to provide an effective relaxation mechanism and effective correlation times are relatively long. Below 110 K molecules stay close to the surface of cages and undergo reorientation in a surface mediated diffusion. Effective correlation time decreases by about three orders of magnitude in a stepwise manner.

The spin-lattice relaxation rate was measured for CD<sub>4</sub> molecules with 4 molecules per supercage in zeolites HY, NaA and NaMord in the range 10 K to 310 K.<sup>23</sup> The transition from translational to rotational mechanism of relaxation was observed at 150 K for HY and at about 200 K for NaA and NaMord zeolites. Also for CD<sub>4</sub> basic features in relaxation are related to quantum effects for free rotators. The theory was fitted in all cases with somewhat different parameters. We report here about HY only for consistency with the principle of common environment.

The relaxation rate depends strongly on the rotational states of CD<sub>4</sub>. These are labelled by the irreducible representations A, T and E of the tetrahedral point group. The symmetry of the total wave functions, being a product of the rotational and spin functions, requires population of rotational states with selected spin isomers A, T and E. Expressions were derived for relaxation rates of magnetizations  $M_T$  and  $M_{AE}$  via the intra- and external quadrupole couplings. Exchange between two locations averages the relaxation rates within the symmetry species. Moreover the spin conversion transitions couple the relaxation of  $M_T$  and  $M_{AE}$ . Two relaxation rates with two maxima in each case were explained with these



postulates. Incoherent tunnelling was attributed to relaxation rates below 15 K.

## Water D<sub>2</sub>O

Applied here methods in analysis of deuteron NMR data, obtained for molecules in confinement, were developed and described before for the case of water.<sup>24</sup> Some of previous results, supplemented by additional measurements, are summarized in Table 1.

Table 1: Water D<sub>2</sub>O.

Sample (loading)	$T_1/T_2$	$T_{50}$ [K]	$T_S$ [K]	$C_Q^{eff}$ [kHz]	$E_a$ [kJ/mol]			
					$T_1$	$R'_1$	$R''_1$	$W$
NaX(1.3) (100%)	14.8	245.0	220.0	143.3	18.6	18.6	$\geq 37.0$	0.3
NaY(1.8) (100%)	42.4	311.0	235.0	241.2	9.0	14.0	30.0	0.75
NaY(2.4) (100%)	36.5	305.0	225.0	87.8	9.8	13.5	$\geq 37.0$	0.115
NaX(1.3) (200%)	59.4	293.0	215.0	139.9	18.4	18.4	$\geq 37.0$	0.3
NaY(2.4) (200%)	9.3	232.5	220.0	162.2	29.1	29.0	$\geq 42.0$	0.4
NaX(1.3) (300%)	24.1	305.0	233.0	136.1	11.4	13.0	$\geq 37.0$	0.3
NaY(1.8) (300%)	10.3	260.0	210.0	139.4	14.3	14.0	$\geq 40.0$	0.28
NaY(2.4) (300%)	8.0	235.0	205.0	149.4	23.3	23.0	$\geq 34.0$	0.33
NaX(1.3) (500%)	24.4	294.0	227.0	133.0	11.0	13.0	$\geq 37.0$	0.27
NaY(2.4), 500%	16.0	250.0	218.0	153.7	31.7 LT	31.5 LT	$\geq 34.0$	0.35 LT
					9.8 HT	36.5 HT		0.15 HT
DY (100%)	37.5	245.0	200.0	148.6	23.0 LT	23.0	$\geq 37.0$	0.32
					9.8 HT			
DY(2.4) (500%)	22.8	240.0	205.0	153.3	23.7 LT	23.0 LT	$\geq 40.0$	0.35 LT
					9.8 HT	18.0 HT		0.3 HT

Two Gaussian components in the spectra were observed in majority of cases. Eventual Lorentzian line at high temperature was considered as a fingerprint of efficient translational motion.

Contributions of Gaussians depend on decreasing temperature, that of narrower one is decreasing. Temperature  $T_{50}$ , where their contributions are equal, was proposed as a parameter related to the adsorption strength; higher when  $T_{50}$  is higher. Inspection of  $T_S$  leads to similar conclusions (Table 1).

Results of direct application of eq 1 in analysis of the spin-lattice relaxation (activation energy and  $C_Q^{eff}$ ) point to necessity of application of the exchange model. High activation energies were attributed to less mobile fraction of molecules. In most cases, irrespective of Si/Al ratio and loading, that fraction dominates (Table 1). All that make water in cationic zeolites a special case. Bonding to the framework at low loading, then formation of clusters are the specific features of water in confinement.

## Ammonia ND<sub>3</sub>

Deuteron NMR spectra and spin-lattice relaxation were measured for the set of zeolites and loadings listed in Table 2. Measurements were performed down to the temperature  $T_S$ , which is significantly higher for NaX than for NaY for respective loadings. Higher  $T_S$  indicates stronger bonding to adsorption centers.

Table 2: Ammonia ND<sub>3</sub>.

Sample loading	$T_1/T_2$	$T_{50}$ [K]	$T_S$ [K]	$E_a$ [kJ/mol]				
				$h$		$R'_1$	$R''_1$	$W$
				HT	LT			
NaX (100%)	197.7	> 260	200	14.5	11	3.9	14.0	0.7
NaX (300%)	107.3	270	210.5	19.2	14.5	3.2	12.7	0.7
NaY (100%)	41.7	250	195	22.1	21.4	5.8	15.2	0.7
NaY (300%)	17.5	190	140	10.4	10.4	5.0	10.0	0.72
DX (100%)	20.0		172	-	-	7.0	20.0	0.88
DY (100%)	$8.5 \cdot 10^3$	-	216	-	-	-	-	-

Analysis of relaxation supplies activation energies. Spectra consist of two components, Gaussian in shape in majority of cases. Linear dependence of their width  $h$  (FWHA) in function of  $1000/T$  indicates Arrhenius process, where the slope defines the activation energy. In some cases two different values were obtained at higher (HT) and lower temperature (LT) (Table 2).

An apparent fit of spin-lattice relaxation rates with eq 1 was possible only in two cases,

NaY (300%) and DY (100%), where a maximum was observed. Reduced values of the quadrupole coupling constant and necessity of finding a common mobility model in all cases leads us to application of the exchange model.

F. Gilles in a scarce paper on ND<sub>3</sub> mobility study by NMR postulated translational jumps between adsorption centers in some Na<sup>+</sup>-faujasites.<sup>25</sup> Ammonia molecules adsorbed in the cationic zeolites interaction with the counter-ions via their nitrogen and deuterons may be involved in hydrogen bonds to the framework oxygens.<sup>26</sup> Both interactions will be considered in analysis of results below. The quadrupole constant for ND<sub>3</sub> was estimated to be 217.5 kHz,<sup>27</sup> or in the range 221.1–239.1 kHz.<sup>25</sup> We take 228 kHz as a common value on the basis of our study.

As the representative example we take the spin-lattice relaxation results for NaY with 300% loading (Figure 1). 3-fold rotation of ammonia reduces the effective quadrupole coupling constant to 76 kHz. The final fit with eq 3 indicates on molecular jumps between two dynamic states described by the relaxation rate  $R'$  with parameters  $\tau'_0 = 2.5 \cdot 10^{-12}$  s,  $E'_a = 5.0$  kJ/mol, and  $R''$  with  $\tau''_0 = 2.0 \cdot 10^{-11}$  s,  $E''_a = 10.0$  kJ/mol. The final fit was obtained for  $W = 0.72$ . The direct fit with eq 1 provided  $C_Q^{eff} = 41.5$  kHz. Results for exchange model for other cationic zeolites are collected in Table 2.

DX zeolite with 100% loading we find as a different case (Figure 2). Here we have:  $R'$  with parameters  $C_Q = 76.0$  kHz,  $\tau'_0 = 2.0 \cdot 10^{-11}$  s,  $E'_a = 7.0$  kJ/mol, and  $R''$  with  $C_Q = 228.0$  kHz,  $\tau''_0 = 1.5 \cdot 10^{-10}$  s,  $E''_a = 20.0$  kJ/mol. Exchange takes place between immobile molecules (static value of  $C_Q$ ) and more abundant rotating molecules (reduced value of  $C_Q$ ) as  $W = 0.88$ . Narrow lines were observed in the whole temperature range.

More restricted mobility of ammonium than in DX was detected in DY. Application of QE sequence was necessary to receive deuteron spectra already at about 300 K. The spectrum obtained at 293 K consists of well defined components (Figure 3). Two Gaussian lines (the shape defined by  $1/(\sigma\sqrt{2\pi}) \exp(-(\nu-\nu_0)^2/(2\sigma^2))$ ) dominate with contributions 40% and 28% and width  $\sigma = 3$  kHz and 9 kHz, respectively. The doublet with contribution 10% comes from

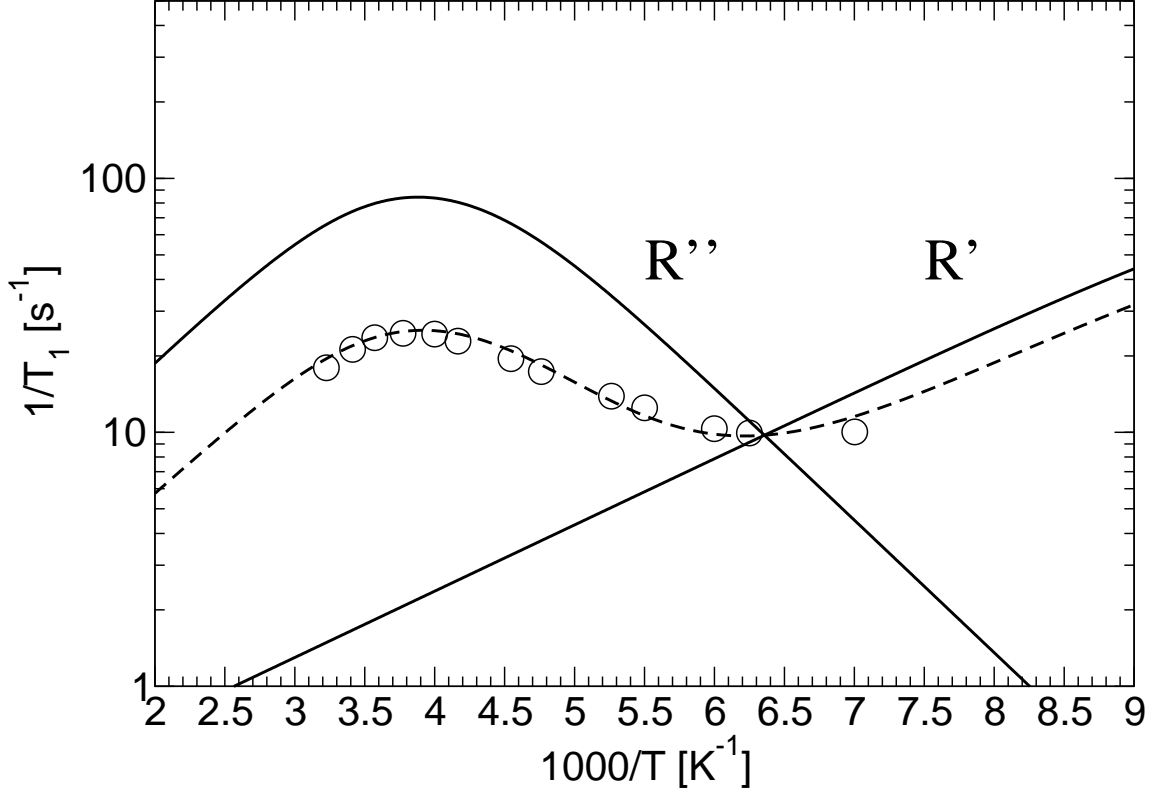


Figure 1: Temperature dependence of deuteron spin-lattice relaxation rate for NaY sample with 300% loading of  $\text{ND}_3$ . Dotted line is relaxation rate  $R$  according to eq 3.

$\text{ND}_3$  undergoing 3-fold rotation. The broad component, contributing 22% of the signal was derived for localized ammonia performing torsional oscillations with  $56^\circ$  amplitude. The spectrum was calculated using WEBLAB package.<sup>28</sup>

The spin-lattice relaxation for DY with 100% loading was also measured using QE sequence (Figure 4) shown together with results for DX (top range) for comparison. Significant difference in  $T_S$  indicates stronger bonding for  $\text{ND}_3$  in DY.

Two time constants above  $T_S$ , the shorter with weight 68% may be attributed to mobile molecules (Gaussians), and the longer one to rotating  $\text{ND}_3$ . Below  $T_S = 216 \text{ K}$  we show, as an example of a common for all cases of molecules in confinement feature, results for localized molecules in DY. Characteristic three time constants, spanned over three orders of magnitude range, indicate on a distribution of correlation times. The conclusion is based on the theoretical procedure worked out before.<sup>29,30</sup>

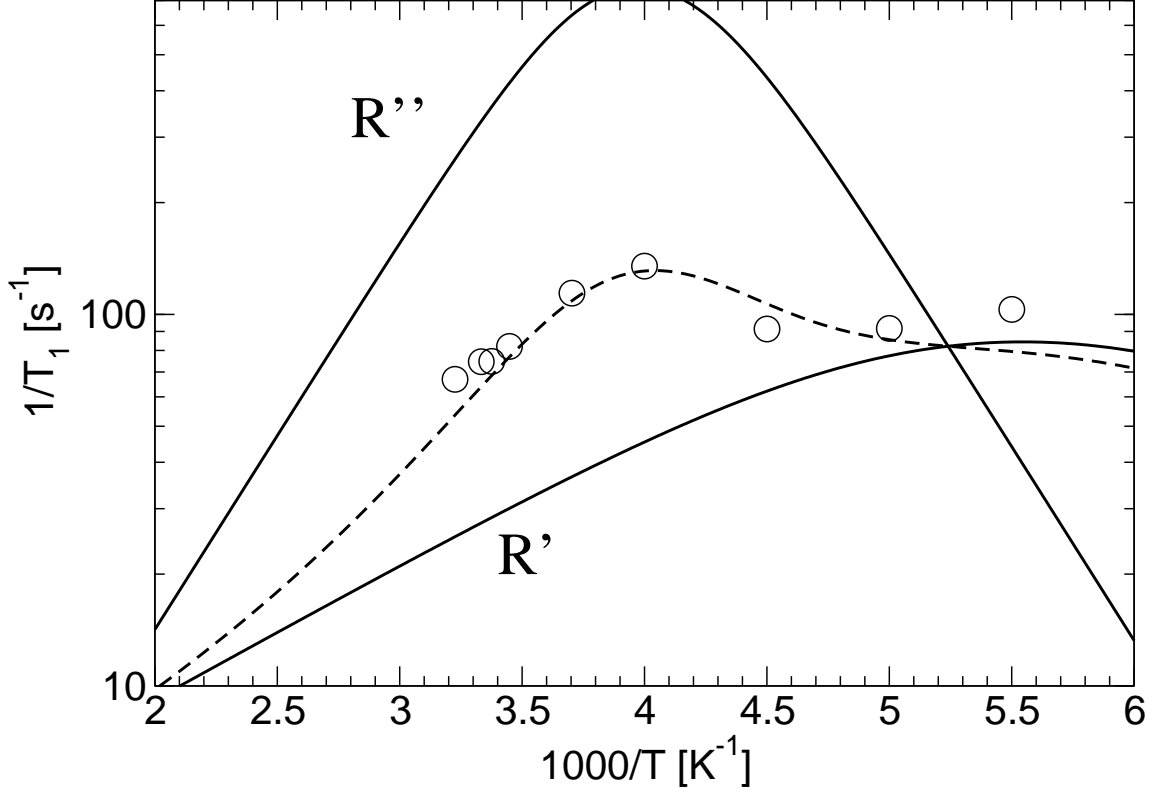


Figure 2: Temperature dependence of deuteron spin-lattice relaxation rate for DX sample with 100% loading of  $\text{ND}_3$ . Dotted line is relaxation rate  $R$  according to eq 3.

As a basic location of ammonia in cationic zeolites one may take the one with molecular nitrogen in the vicinity of the cation. The hydrogen bond of molecular deuteron with a framework oxygen is also possible (Figure 2 in Ref.<sup>25</sup>).

Electrical charge of  $\text{Na}^+$  in NaY is stronger and nitrogen bonding stronger than in NaX. Activation energies from  $R''$  (Table 2) do not confirm that expectation clearly enough. On the other hand however, inspection of  $T_S$  temperatures corroborate importance of N- $\text{Na}^+$  interaction.

Experimental results indicate that molecular mobility in DX and DY appears to be significantly different. The structure with ammonia nitrogen at the framework deuterium may be seen as formation of a quasi-ammonium ion. Such singly bonded state<sup>31,32</sup> allows free 3-fold rotation of ammonia and appears to be more abundant in NaX. Triply bonded structure (Figure 6c in Ref.<sup>31</sup>) refer to localized, performing torsional oscillations ammonia

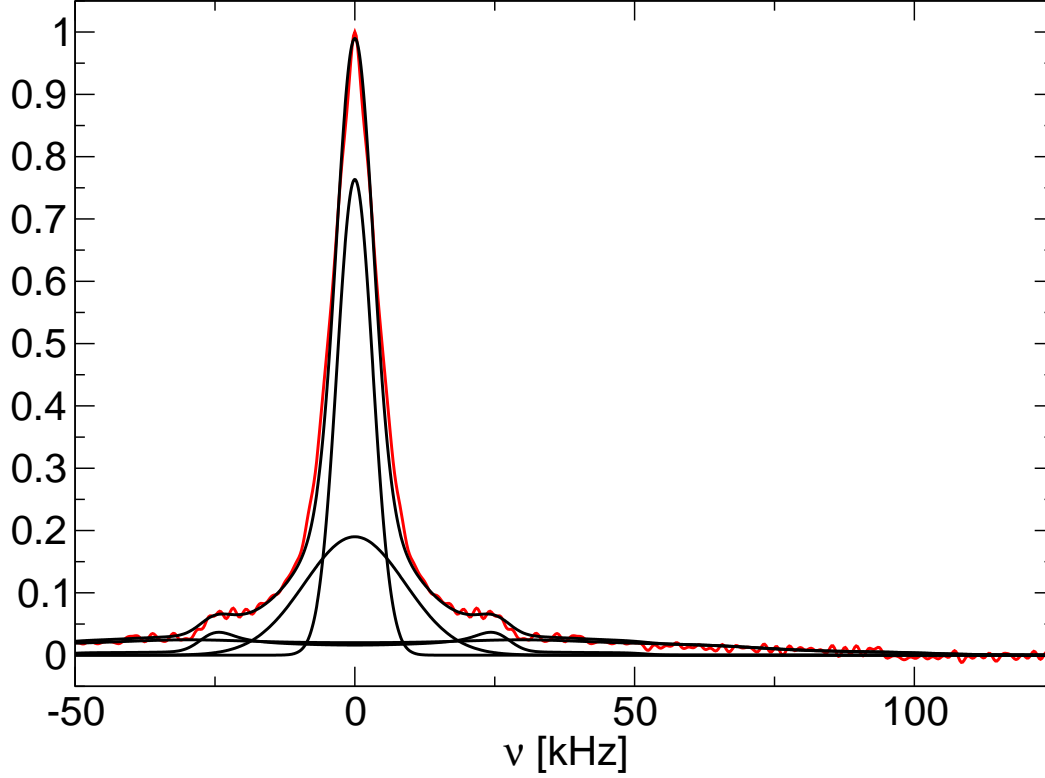


Figure 3: Deuteron spectrum of ammonia confined in DY zeolite at 100%  $\text{ND}_3$  loading level. Spectral components resulting from the numerical decomposition of the total spectra are shown.

in a strong potential with the 3-fold symmetry.

Hydrogen bonds are relatively weaker in DY, however the exchange model was not applicable in this case. Majority of molecules (Gaussian components amount to 68%) perform almost isotropic reorientation, however with highly restricted translational diffusion. Just a fraction is fully localized with the single bond (3-fold rotation) or triply bonded (torsional oscillations). The loading 100% means that we have 86 or 56 molecules in the unit cell in DX and DY, respectively. It leads to an additional concept that more frequent collisions between more abundant molecules in the space of DX cages may overshadow features related to bonding and settle the final view of molecular mobility in confinement.

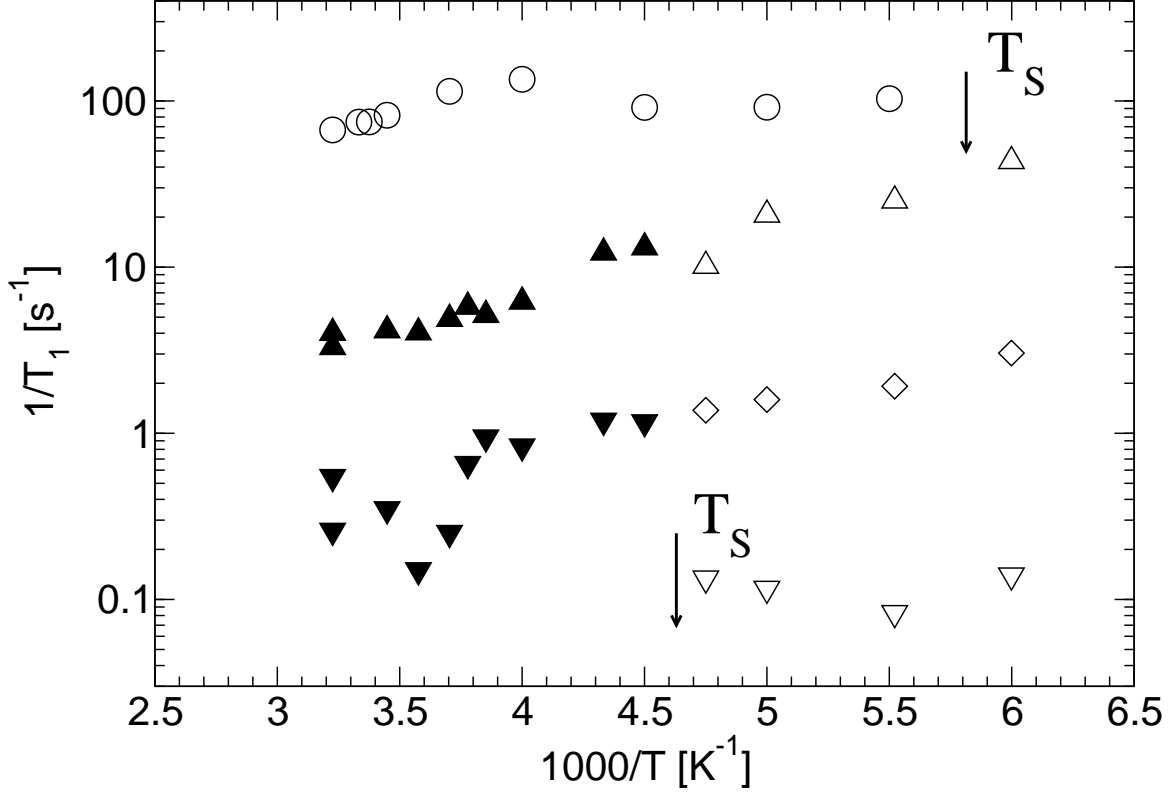


Figure 4: Temperature dependence of deuteron spin-lattice relaxation rate for DY sample with 100% loading of  $\text{ND}_3$ . The circles are for DX sample with 100% loading of  $\text{ND}_3$ .

### Methanol $\text{CD}_3\text{OD}$

As the key example we take NaY zeolite with 100% loading. Two time constants are observed in the temperature dependence of the spin-lattice relaxation (Figure 5). The higher relaxation rate was fitted with  $C_Q^{\text{eff}} = 142.6 \text{ kHz}$  in eq 1. At about 260 K its contribution comes to zero from about 25% at highest temperature. The slower relaxation rate, characterized by  $C_Q^{\text{eff}} = 28.3 \text{ kHz}$  is dominating down to  $T_S = 215 \text{ K}$ . At this point spectrum broadens significantly, indicating immobilization of all molecules.

In the case of NaX with 100% loading  $T_S$  temperature is lower than for NaY and equals 190 K (Table 3, Ref.<sup>33</sup>), thus the binding energy is lower. From relaxation between binding energies we may point out the location of methanol molecules with oxygens at  $\text{Na}^+$  cations, as their electrical charge is higher in NaY compared to NaX. Thus the first adsorption layer consists of molecules at so called horizontal position.<sup>33</sup> The conclusion directs us to an

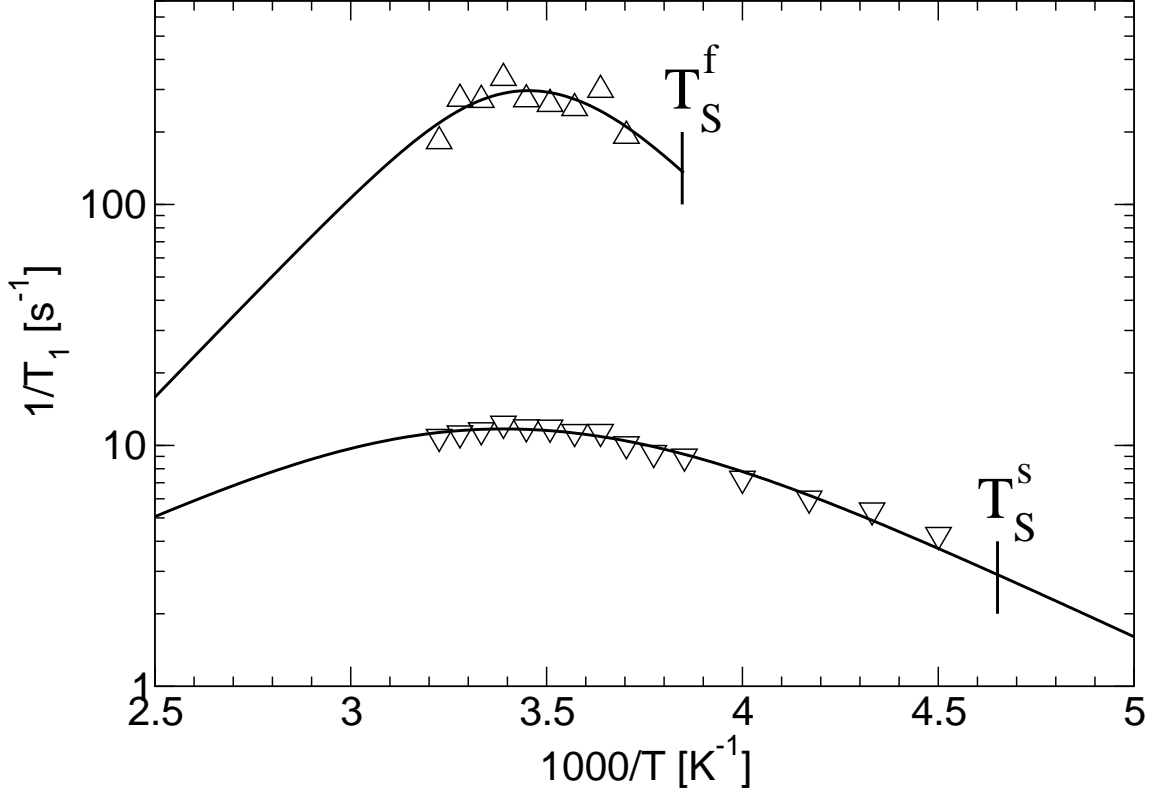


Figure 5: Temperature dependence of deuteron spin-lattice relaxation rate for NaY sample with 100% loading of  $\text{CD}_3\text{OD}$ . Symbols  $\triangle$ , and  $\nabla$ , are fast and slow relaxation rates, respectively.

expalantion of oberved relaxation rates based on a common view of molecular mobility. A fractional methanol molecules face a reduced mobility in a sort of first adsorption layer in the vicinity of  $\text{Na}^+$  cations. The fast relaxation rate, with high  $C_Q^{eff}$  value, is driven by rotating OD and  $\text{CD}_3$  groups in absence of any overall reorientation. Increasing width of spectra eliminates that time constant from detection using FID below 260 K.

The slower relaxation rate refers to majority of molecules moving freely in the space of cages, performing isotropic reorientations accompanied with internal fast rotations of both OD and  $\text{CD}_3$ . Solidification temperatures for molecules contributing to the fast and slow relaxation rates, 260 K and 215 K, respectively, are resulting from difference in binding energy (respective activation energies are equal 32.3 kJ/mol and 14.5 kJ/mol (Table 3). There are two exponents in the spectra, narrow and broader, being referred to as N and B in Table 3, respectively. Contributions of the narrow and broader components amount to about 40% and



Table 3: Methanol CD<sub>3</sub>OD.

Sample, l.	$T_1/T_2$	$T_{50}$ [K]	$T_S$ [K]	$C_Q^{eff}$	$E_a$ [kJ/mol]				W
					$T_1$	l. width	$R'_1$	$R''_1$	
NaX, 100%	110.3 N	250.0	190.0	123.0	20.7	-			
	20.1 B			24.3	8.6	-			
NaY, 100%	18.7 N	260.0	215.0	142.6	32.3	31.2 N			
	2.7 B			28.3	14.5	23.4 B			
NaX, 200%	128.4 N	-	166.7	-	12.7 OD	-	14.0 OD	13.0 OD	0.3
	304.2 B			-	10.4 CD <sub>3</sub>	-	14.0 CD <sub>3</sub>	13.0 CD <sub>3</sub>	0.3
NaY, 200%	-	-	153.8	120.8	9.7 OD	-	13.3 OD	18.3 OD	0.35
	-			-	11.3 CD <sub>3</sub>	-	13.0 CD <sub>3</sub>	18.0 CD <sub>3</sub>	0.35

60% at higher temperature. The contribution of the broader exponent increases significantly below  $T_{50} = 260$  K. The width of the narrow component does not change significantly in the whole range of temperature, while for the broader component a continuous increase is observed (Figure 6).

The comprehensive view of molecular mobility in confinement must involve the basic assumption of a broad distribution of correlation time. As pointed out above we have  $\tau_c = 10^{-6}$  s as boundary condition for narrowing of deuteron spectra. Molecules with longer  $\tau_c$  contribute broad lines, alternative those with shorter provide narrow lines, thus using FID method we detect signal from a fraction of molecules with higher mobility. Application of QE methods would be necessary in order to get a complete view with both fractions of molecules.

The features observed in relaxation at 200% loading are substantially different. Existence of methanol trimers was the key point in explaining them.

## Acetone (CD<sub>3</sub>)<sub>2</sub>CO

Relaxation rates are shown in Figure 7 and 8 for NaX and NaY, respectively. There are significant differences, however no obvious interpretation appears. We may search for differences in molecular mobility in deuteron spectra below  $T_S$ . Rotation of methyl groups takes

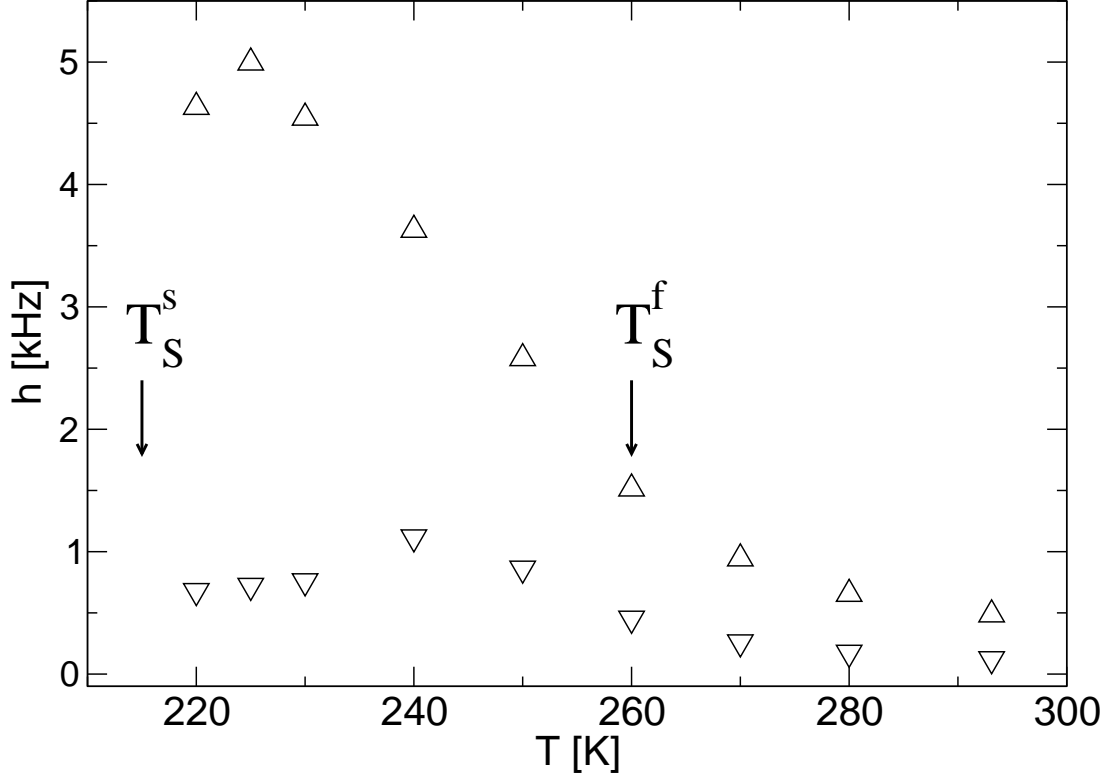


Figure 6: NaY sample with 100% loading of  $\text{CD}_3\text{OD}$ . Temperature dependence of spectral width  $h$  (FWHA) for narrow ( $\nabla$ ) and broad ( $\triangle$ ) Gaussian lineshapes, respectively.

place down to low temperature. Therefore, in the temperature range considered here, its contribution to relaxation is negligible.

Mobility of acetone molecule consists of torsional oscillations about the 2-fold symmetry axis ( $z$ ), the axis in the molecular plane ( $y$ ), and about the axis perpendicular to the plane ( $x$ ). Oscillations are induced on increasing temperature in this order. All of them are effective in NaX just below  $T_S$ . Therefore we may expect above  $T_S$  uniform isotopic reorientations of acetone molecules. The maximum in spin-lattice relaxation rate provides the activation energy 9.2 kJ/mol.

Spectral component related to 2-fold oscillations dominate in the spectra of NaY just below  $T_S$ . Another one with about 15% contribution indicates on consecutive oscillations about  $z$  and  $y$  axes. Acetone molecules are subjected to hindrance by a local potential with lower symmetry in this case. The time constants in the spin-lattice relaxation rate

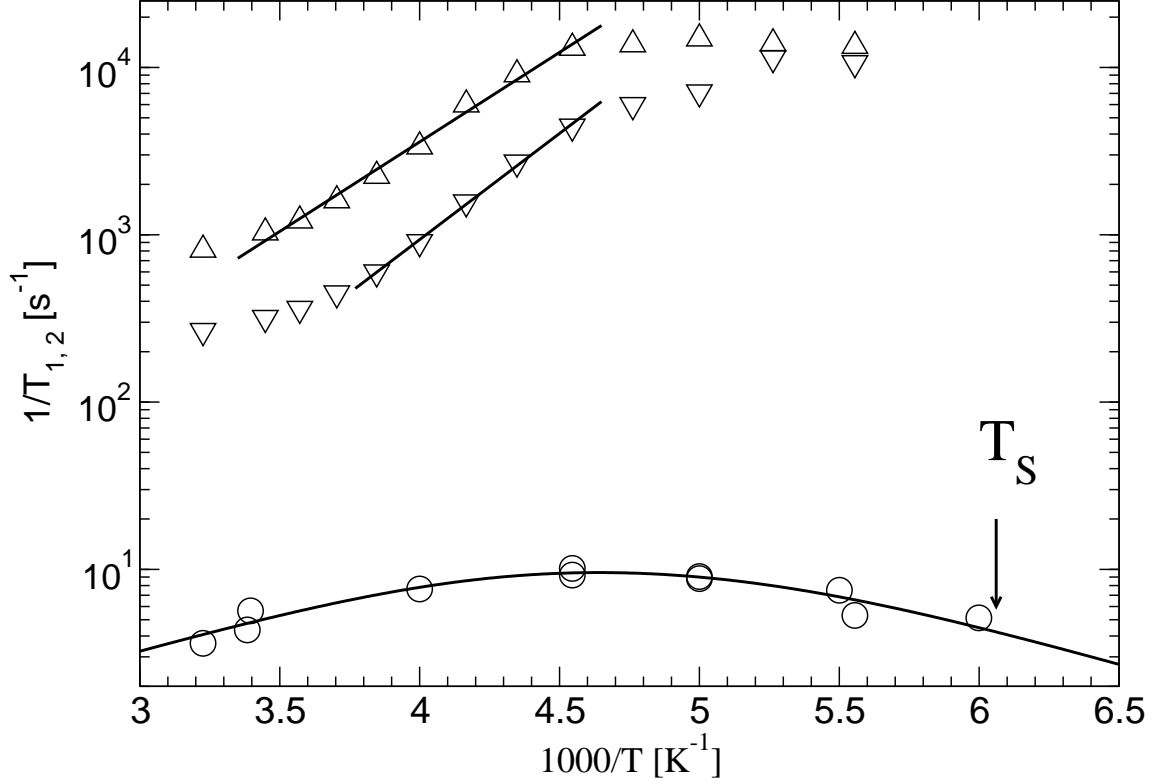


Figure 7: Temperature dependence of deuteron relaxation rates  $R_1$  and  $R_2$  for NaX sample with 100% loading of  $(\text{CD}_3)_2\text{CO}$ . Symbols  $\circ$ , and  $\triangle$ ,  $\nabla$ , refer to spin-lattice  $R_1$  and spin-spin  $R_2$  relaxation rates, respectively.

reflect complexity of molecular dynamics above  $T_S$ , where 2-fold oscillations may evolve into rotational jumps. Their weights, 85% and 15% for shorter and longer one in the whole temperature range, respectively confirm domination of mobility about  $z$  axis, accompanied by rotational mobility also about  $y$  axis for the fraction of molecules.

Spectra are composed of two Gaussians. Their width shows in significant temperature dependence (Figure 8). Alternatively for NaX spectra are broader and high activation energy was derived (Table 4). Exchange of methyl groups in acetone via 2-fold rotation was proposed before.<sup>34</sup> Extensive studies of acetone adsorption were performed using  $^{13}\text{C}$  chemical shift.<sup>35,36</sup> A relation was found between the  $^{13}\text{C}$  chemical shift and acid strength of Brønsted and Lewis acid sites. Effects of molecular reorientations were detected.<sup>36</sup> When acetone adsorbs on Lewis acid sites, the carboxyl oxygen of acetone interacts with the Al atom of the zeolite framework to form a coordination adsorption complex. Such geometry is basic

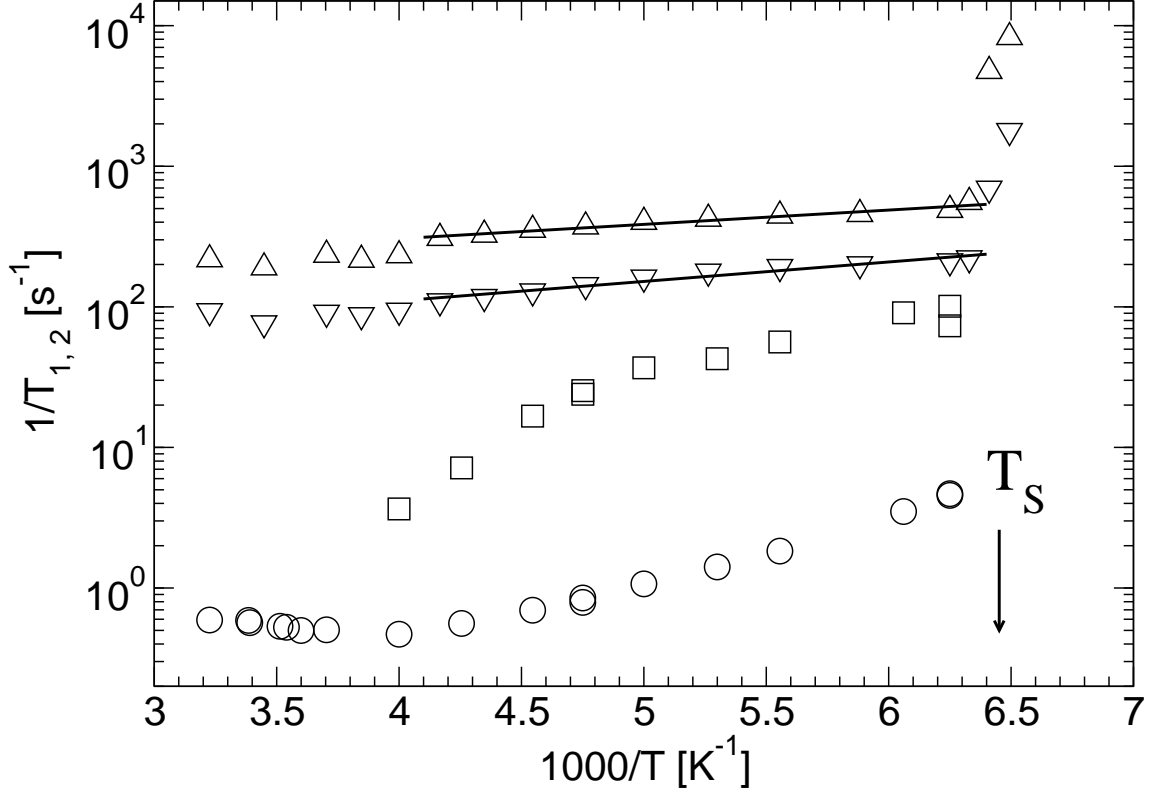


Figure 8: Temperature dependence of deuteron relaxation rates  $R_1$  and  $R_2$  for NaY sample with 100% loading of  $(\text{CD}_3)_2\text{CO}$ . Symbols  $\circ$ ,  $\square$  and  $\triangle$ ,  $\nabla$ , refer to spin-lattice  $R_1$  and spin-spin  $R_2$  relaxation rates, respectively.

in the case of NaX and NaY. Molecular reorientations and their activation energy as well as  $T_S$  indicate on stronger interaction of acetone with Lewis sites in the case of NaY (Table 4).

Table 4: Acetone  $(\text{CD}_3)_2\text{CO}$ .

Sample, loading	$T_1/T_2$	$T_{50}$ [K]	$T_S$ [K]	$E_a$ [kJ/mol]				W
				$T_1$	line width	$R'_1$	$R''_1$	
NaX, 100%	206.0	255	165	9.2	20.5	9.2	37.0	0.12
	74.5				24.3			
NaY, 100%	-	250	155	-	21.0	8.7	25.0	0.15

## Translation to rotation transition

Spin-lattice relaxation rates are consistent with the model of the fast magnetization exchange between two dynamically different deuteron populations. Effective correlation times are long ( $\omega_0\tau_c \gg 1$ ) and the low temperature slope is observed. The observed relaxation behaviour in temperature dependence is most likely an effect of the transition from translational to rotational diffusion as the major relaxation mechanism. In the transition may be visualized as a transfer from surface free (collisions) to surface mediated (molecules rolling over the surface of cages) diffusion. A change in effective correlation time by three or four orders of magnitude stays behind the transition in terms of relaxation efficiency.

Table 5: Translation to rotation transition temperature  $T_{TR}$  [K]

	NaX	NaY	HY/DY	NaA
D <sub>2</sub>		110.0		
CD <sub>4</sub>			150.0	200.0
D <sub>2</sub> O (100%)	318.0	322.6	34.1	
D <sub>2</sub> O (200%)	335.6	342.5		
D <sub>2</sub> O (300%)	333.3	304.9		
D <sub>2</sub> O (500%)	333.3	343.6	327.9	
ND <sub>3</sub> (100%)	261.0	235.0	191.0	
ND <sub>3</sub> (300%)	259.0	157.0		
CD <sub>3</sub> OD (200%)	245.0	230.0		
(CD <sub>3</sub> ) <sub>2</sub> CO (100%)	416.6	266.6		

## Conclusion

Applicability of deuteron NMR methods in studies of molecular mobility was tested on a series of molecules confined in cages of zeolites with the faujasite structure. Several parameters related to their interaction, mutual and with the zeolite framework, were obtained and compared. Each case appears to be the unique one. Obtained parameters reflect distinct influence of adsorption centers and, on increasing loading, also on variety of mutual

interactions. Particularly formation of molecular aggregates like water clusters or assembling of ammonia gave most rewarding features in deuteron NMR observables. All together supplies guidance for future applications of deuteron NMR in studies of molecular dynamics in confinement and proofs it to be the useful tool.

## Acknowledgement

The work was financed by the National Centre for Research and Development, contract No. PBS2/A2/16/2013.

## References

- (1) Buntkowsky, G.; Breitzke, H.; Adamczyk, A.; Roelofs, F.; Emmmler, T.; Gedat, E.; Grünberg, B.; Xu, Y.; Limbach, H.-H.; Shenderovich, I.; Vyalikh, A.; Findenegg, G. Structural and dynamical properties of guest molecules confined in mesoporous silica materials revealed by NMR. *Phys. Chem. Chem. Phys.* **2007**, *9*, 4843–4853.
- (2) Werner, M.; Rothermel, N.; Breitzke, H.; Gutmann, T.; Buntkowsky, G. Recent Advances in Solid State NMR of Small Molecules in Confinement. *Isr. J. Chem.* **2014**, *54*, 60–73.
- (3) Ashbrook, S. E.; Dawson, D. M. Recent developments in solid-state NMR spectroscopy of crystalline microporous materials. *Phys. Chem. Chem. Phys.* **2014**, *16*, 8223–8242.
- (4) Meier, W. M.; Olson, D. H. *Atlas of Zeolite Structure Types*, 3rd ed.; Butterworth: London, 1992.
- (5) Kobe, J. M.; Gluszak, T. J.; Dumesic, J. A.; Root, T. W. Deuterium NMR Characterization of Brønsted Acid Sites and Silanol Species in Zeolites. *J. Phys. Chem.* **1995**, *99*, 5485–5491.

- (6) Czjzek, M.; Jobic, H.; Fitch, A. N.; Voigt, Th. Direct determination of proton positions in D-Y and H-Y zeolite samples by neutron powder diffraction. *J. Phys. Chem.* **1992**, *96*, 1535–1540.
- (7) Dubsky, J.; Bera, S.; Bosáček, V. Quantum chemical calculations of the physical characteristics of the hydroxyl groups of zeolites. *J. Mol. Catal.* **1979**, *6*, 321–326.
- (8) Schröder, K.-P.; Sauer, J.; Leslie, M.; Richard, C.; Catlow, A.; Thomas, J. M. Bridging hydroxyl groups in zeolitic catalysts: a computer simulation of their structure, vibrational properties and acidity in protonated faujasites (H-Y zeolites). *Chem. Phys. Lett.* **1992**, *188*, 320–325.
- (9) Stoch, G.; Ylinen, E. E.; Punkkinen, M.; Petelenz, B.; Birczyński, A. Deuteron NMR spectra and relaxation in fully and partly deuterated  $(\text{NH}_4)_2\text{ZnCl}_4$ . *Solid State Nucl. Magn. Reson.* **2009**, *35*, 180–186.
- (10) Abragam, A. *The Principles of Nuclear Magnetism*; Oxford University Press: Oxford, UK, 1961, Chap. VIII.
- (11) Zimmerman, J. R.; Brittin, W. E. Nuclear Magnetic Resonance Studies in Multiple Phase Systems: Lifetime of a Water Molecule in an Adsorbing Phase on Silica Gel. *J. Chem. Phys.* **1957**, *61*(10), 1328–1333.
- (12) Szymocha, A. M.; Birczyński, A.; Lalowicz, Z. T.; Stoch, G.; Krzystyniak, M.; Góra-Marek, K. Water Confinement in Faujasite Cages: A Deuteron NMR Investigation in a Wide Temperature Range. 1. Low Temperature Spectra. *J. Phys. Chem. A* **2014**, *118*, 5359–5370.
- (13) Slichter, C. P. *Principles of Magnetic Resonance*, 3rd ed.; Springer-Verlag: New York, 1990.

- (14) Schmidt-Rohr, K.; Spiess, H. W. *Multidimensional Solid-State NMR and Polymers*; Academic Press: New York, 1994.
- (15) Mehring, M. *Principles of High Resolution NMR in Solids*; Springer Verlag: New York, 1983.
- (16) Ylinen, E. E.; Lalowicz, Z. T.; Sagnowski, S. F.; Punkkinen, M.; Koivula, E.; Ingman, L. P. Deuteron NMR Spectrum of  $\text{ND}_4\text{VO}_3$  and Some Other Ammonium Compounds. *Chem. Phys. Lett.* **1992**, *192*, 590–594.
- (17) Grünberg, B.; Emmler, Th.; Gedat, E.; Shenderovich, I.; Findenegg, G. H.; Limbach, H.-H.; Buntkowsky, G. Hydrogen Bonding of Water Confined in Mesoporous Silica MCM-41 and SBA-15 Studied by  $^1\text{H}$  Solid-State NMR. *Chem. Eur. J.* **2004**, *10*, 5689–5696.
- (18) Rössler, E.; Taupitz, M.; Börner K.; Schulz, M.; Vieth, H.-M. A Simple Method Analyzing  $^2\text{H}$  Nuclear Magnetic Resonance Line Shapes to Determine the Activation Energy Distribution of Mobile Guest Molecules in Disordered Systems. *J. Chem. Phys.* **1990**, *92*, 5847–5855.
- (19) Bloom, M.; Davis, J. H.; Valic, M. I. Spectral distortion effects due to finite pulse widths in deuterium nuclear magnetic resonance spectroscopy. *Can. J. Phys.* **1980** *58* 1510–1517.
- (20) Stoch, G.; Olejniczak, Z. Missing First Points and Phase Artifact Mutually Entangled in FT NMR Data – Noniterative Solution. *J. Magn. Reson.* **2005**, *173*, 140–152.
- (21) Heuer, A.; Haeberlen, U. A New Method for Suppressing Baseline Distortions in FT NMR. *J. Magn. Reson.* **1989**, *85*, 79–94.



- (22) Blicharski, J. S.; Gutsze, A.; Korzeniowska, A. M.; Lalowicz, Z. T.; Olejniczak, Z. Deuteron Spin-Lattice Relaxation Study of D<sub>2</sub> Secluded in the Supercages of Zeolite NaY. *Appl. Magn. Reson.* **2004**, *27*, 183–195.
- (23) Birczyński, A.; Punkkinen, M.; Szymocha, A. M.; Lalowicz, Z. T. Translational and reorientation of CD<sub>4</sub> molecules in nanoscale cages of zeolites as studied by deuteron spin-lattice relaxation. *J. Chem. Phys.* **2007**, *127*, 204714 (10pp).
- (24) Szymocha, A. M.; Lalowicz, Z. T.; Birczyński, A.; Krzystyniak, M.; Stoch, G.; Góra-Marek, K. Water Confinement in Faujasite Cages: A Deuteron NMR Investigation in a Wide Temperature Range. 2. Spectra and Relaxation at High Temperature. *J. Phys. Chem. A* **2014**, *118*, 5371–5380.
- (25) Gilles, F.; Blin, J.-L.; Su, B.-L. Transport properties of ammonia in a series of Na<sup>+</sup>-faujasite zeolites as studied by <sup>2</sup>H NMR technique. *Colloid Surface A* **2004**, *241*, 253–256.
- (26) Gilles, F.; Blin, J.-L.; Toufar, B.; Briend, M.; Su, B. L. Double interactions between ammonia and a series of alkali-exchanged faujasite zeolites evidenced by FT-IR and TPD-MS techiques. *Colloid Surface A* **2004**, *241*, 245–252.
- (27) Rabideau, S. W.; Waldstein, P. Deuteron Magnetic Resonance of Polycrystalline Deuteroammonia. *J. Chem. Phys.* **1966**, *45*(12), 4600–4603.
- (28) Macho, V.; Brombacher, L.; Spiess, H. W. The NMR-WEBLAB: an Internet Approach to NMR Lineshape Analysis. *Appl. Magn. Reson.* **2001**, *20*, 405–432.
- (29) Stoch, G.; Ylinen, E. E.; Birczyński, A.; Lalowicz, Z. T.; Góra-Marek, K.; Punkkinen, M. Deuteron spin-lattice relaxation in the presence of an activation energy distribution: Application to methanols in zeolite NaX. *Solid State Nucl. Magn. Reson.* **2013**, *49–50*, 33–41.

- (30) Ylinen, E. E.; Punkkinen, M.; Birczyński, A.; Lalowicz, Z. T. The effect of a broad activation energy distribution on deuteron spin-lattice relaxation. *Solid State Nucl. Magn. Reson.* **2015**, *71*, 19–29.
- (31) Jacobs, W. P. J. H.; de Haan, V. O.; van Santen, R. A.; de Graaf, L. A. A Quasi-Elastic Neutron Scattering Study of the Ammonia Ions in CsNH<sub>4</sub>-Y Zeolite. *J. Phys. Chem.* **1994**, *98*, 2180–2184.
- (32) Brändle, M.; Sauer, J. Combining ab initio techniques with analytical potential functions. A study of zeolite-adsorbate interactions for NH<sub>3</sub> on H-faujasite. *J. Mol. Catal. A-Chem.* **1997**, *119*, 19–33.
- (33) Lalowicz, Z. T.; Stoch, G.; Birczyński, A.; Punkkinen, M.; Ylinen, E. E.; M.; Petelenz, B.; Krzystyniak, M.; Góra-Marek, K.; Datka, J. Translational and rotational mobility of methanol-d<sub>4</sub> molecules in NaX and NaY zeolite cages: A deuteron NMR investigation. *Solid State Nucl. Magn. Reson.* **2012**, *45–46*, 66–74.
- (34) Udachin, K. A.; Enright, G. D.; Ratcliffe, C. I.; Ripmeester, J. A. Locating Dynamic Species with X-ray Crystallography and NMR Spectroscopy: Acetone in p-tert-Butylcalix[4]arene. *ChemPhysChem* **2015**, *4*, 1059–1064.
- (35) Fang, H.; Zheng, A.; Chu, Y.; Deng, F. <sup>13</sup>C Chemical Shift of Adsorbed Acetone for Measuring the Acid Strength of Solid Acids: A Theoretical Calculation Study. *J. Phys. Chem. C* **2010**, *114*, 12711–12718.
- (36) Biaglow, A. I.; Gorte, R. J.; White, D. Molecular Motions and <sup>13</sup>C Chemical Shift Anisotropy of Acetone Adsorbed in H-ZSM-5 Zeolite. *J. Phys. Chem.* **1993**, *97*, 7135–7137.

